Available online at www.sciencedirect.com
SCIENCE DIRECT
Journal of Power Sources 153 (2006) 165–169
JOURNAL OF POWER SOURCES
www.elsevier.com/locate/jpowsour

Short communication

Lithium insertion into manganese dioxide electrode in MnO_2/Zn aqueous battery Part III. Electrochemical behavior of γ-MnO_2 in aqueous lithium hydroxide electrolyte

Manickam Minakshi [a,*], Pritam Singh [a], Touma B. Issa [a], Stephen Thurgate [a], Roland De Marco [b]

[a] *Division of Science and Engineering, Murdoch University, Murdoch 6150, WA, Australia*
[b] *Department of Applied Chemistry, Curtin University of Technology, Bentley 6102, WA, Australia*

Received 30 January 2005; accepted 11 March 2005
Available online 31 May 2005

Abstract

The electrochemical behavior of γ-MnO_2 in lithium hydroxide (LiOH) and potassium hydroxide (KOH) aqueous media has been studied using slow-scan cyclic voltammetry (25 μV s^{-1}) in conjunction with X-ray analysis (XRD) and scanning electron microscopy (SEM). The reduction of γ-MnO_2 in aqueous LiOH results in intercalation of Li^+ forming a new phase of lithium intercalated MnO_2 (Li_xMnO_2). The process is found to be reversible. In this regard, the reduction of γ-MnO_2 in LiOH is quite different from that in aqueous KOH, which is irreversible and no lithium intercalation occurs. This difference in behavior is explained in terms of the relative ionic sizes of Li^+ and K^+. The Li_xMnO_2 lattice is stable only for Li^+ because Li^+ and Mn^{4+} are of approximately the same size whereas K_xMnO_2 is not stable because K^+ has almost double the size.

Keywords: Cyclic voltammetry (CV); γ-MnO_2; Lithium insertion; Rechargeability; Ionic size; Aqueous battery

1. Introduction

Manganese dioxide (MnO_2) is commonly used as a cathode in aqueous zinc/MnO_2 batteries, which use KOH as the electrolyte. MnO_2 undergoes reduction through a mechanism involving proton insertion into the MnO_2 structure. In a recent paper [1], we reported that when MnO_2 is discharged in cells containing aqueous LiOH electrolyte the mechanism is quite different, i.e. instead of H^+ insertion Li^+ intercalation into the lattice of the host γ-MnO_2 occurs. This intercalation was shown to be reversible. This finding is interesting because it opens up a new field of aqueous batteries utilizing rechargeable γ-MnO_2 cathode.

In this paper, we report the results of a subsequent study, specifically focusing on the mechanism of the intercalation reaction. A cyclic voltammetric (CV) study together with characterization by specialist techniques like X-ray diffraction (XRD) and scanning electron microscope (SEM) of the materials that are formed during the electrochemical discharge of γ-MnO_2 is carried out.

2. Experimental

The cell design, experiment details, and the method of preparing X-ray, XPS and IR samples have been described elsewhere [1,2].

2.1. Slow-scan cyclic voltammetry

For cyclic voltammetric experiments, a three-electrode cell was used. The working electrode, consisted of a disk

* Corresponding author. Tel.: +61 8 9360 2379; fax: +61 8 9310 1711
E-mail addresses: minakshi@murdoch.edu.au (M. Minakshi), p.singh@murdoch.edu.au (P. Singh).

0378-7753/$ – see front matter © 2005 Elsevier B.V. All rights reserved.
doi:10.1016/j.jpowsour.2005.03.184

(12 mm diameter with 1 mm thickness), γ-MnO_2 mixed with conductive carbon (A-99, Asbury, USA). This disk was embedded into a Pt gauze through which the electric contact was made. The counter electrode was a Zn foil, which was separated from the main electrolyte by means of a porous frit. A saturated calomel electrode (SCE) served as the reference electrode. The electrolyte was a saturated solution of lithium hydroxide. The working electrode was cycled between 0.4 and −0.6 V at 25 μV s^{-1} scan rate. On each occasion the potential scan started at 0.4 V, moving initially in the cathode direction. At appropriate points of the experiment, the cathode material was removed from the solution, washed with water and characterized by XRD and SEM analysis. All the cyclic voltammetric experiments were done by using EG&G Princeton Applied Research Potentiostat/Galvanostat model 273A, operated by model 270 software (EG&G). All potentials were measured with respect to a saturated calomel electrode. All the electrochemical measurements were carried out at ambient room atmosphere (25 ± 1 °C).

The products formed during the cathodic scan were characterized by X-ray diffraction and scanning electron microscopy. For X-ray analysis a Siemens X-ray diffractometer using Philips Co Kα radiation was used. A (Philips Analytical XL series 20) scanning electron microscope was used for surface analysis investigations.

3. Results and discussion

Fig. 1 shows the first cyclic voltammogram of γ-MnO_2 under the conditions noted in the figure. As can be seen in Fig. 1, the CV profile consists of a reduction peak C_1 at −480 mV and its corresponding anodic peak A_1 at −160 mV. A small shoulder at 46 mV is also seen during the scan in the anodic direction.

Fig. 2 shows the changes in the CV profile when the material is subjected to continuous cycling (20 cycles) in the potential region +0.4 to −0.6 V. The cathodic and anodic peak currents decreased slightly up to about 10 cycles and then tended to stabilize suggesting that the material could be reversibly reduced/oxidized over a number of cycles. To confirm that the anodic peak corresponded to the reduction reaction at −480 mV, the following experiment was done. The γ-MnO_2 was scanned cathodically up to −480 mV and then held constant at that point over 20, 40 and 60 min. At the end of the holding potential, the scan was reversed and the anodic peak current measured. The data is shown in Fig. 3. Clearly, as the time for which the electrode is held at constant potential (−480 mV) the corresponding anodic peak current increases. This observation confirms that the electro reduction of γ-MnO_2 was reversible. The ratio of the charge under the peaks C_1 and A_1 is 0.81 suggesting that the reaction is 81% reversible.

There is a substantial body of literature [3–6] relating to performance characteristics of MnO_2 in alkaline aqueous

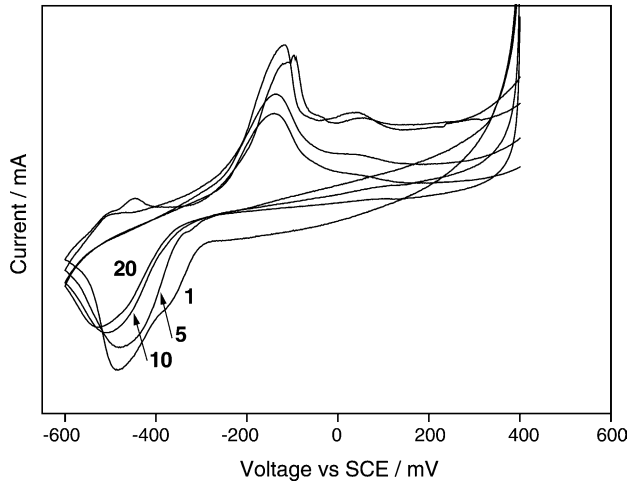

Fig. 2. Cyclic voltammogram of γ-MnO_2 in LiOH for the repeated cycles, potential scanned at 25 μV s^{-1} from +0.4 to −0.6 V and back.

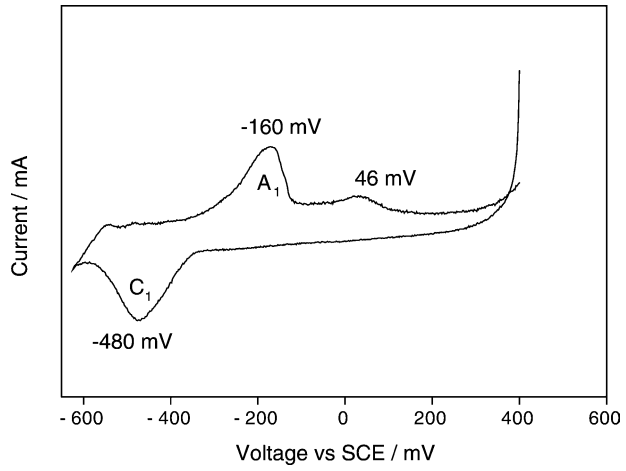

Fig. 1. Cyclic voltammogram of γ-MnO_2 in LiOH for the first cycle, potential scanned at 25 μV s^{-1} from +0.4 to −0.6 V and back.

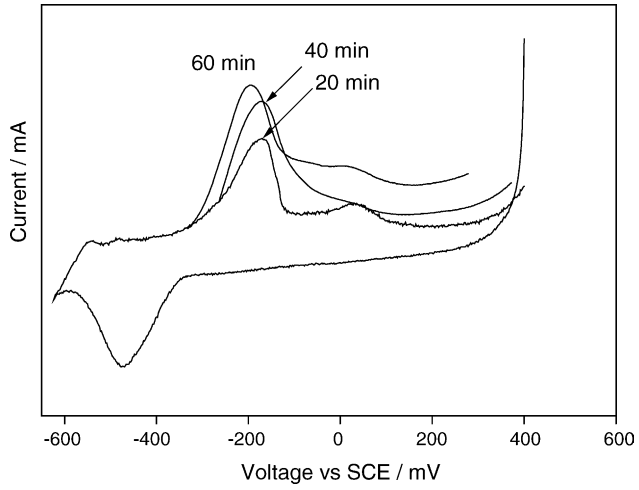

Fig. 3. Cyclic voltammogram of γ-MnO_2 in LiOH, potential held at −480 mV. Time in figure indicates the (holding time) lithium concentration.

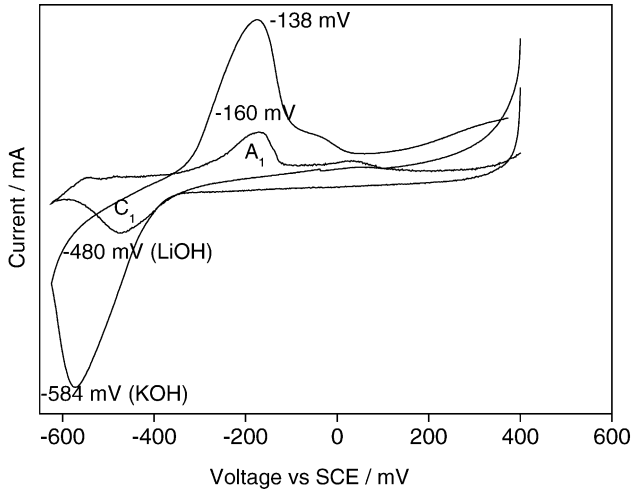

Fig. 4. Cylic voltammogram of γ-MnO_2 in KOH for the potential scanned at 25 μV s^{-1} from +0.4 to −0.6 V and back.

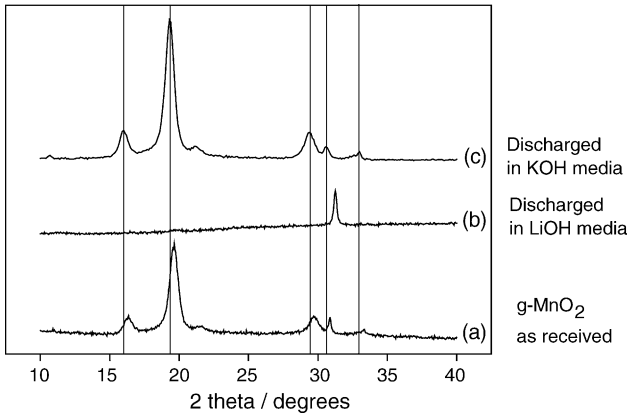

Fig. 5. X-ray diffraction patterns changes of γ-MnO_2 after the cyclic voltammetry studies in an aqueous battery (a) γ-MnO_2 (before discharge), (b) reduced at −480 mV in LiOH media and (c) reduced at −584 mV in KOH media.

MnO_2 cells containing potassium hydroxide (KOH) as the electrolyte. The behavior of the MnO_2 in aqueous LiOH can be compared to KOH by referring Fig. 4. The data for both the electrolyte were obtained under identical conditions. The CV's of MnO_2 in the two electrolytes are quite different. While, the reduction peak in KOH occurs at −584 mV, the cathodic peak in the presence of LiOH is at −480 mV. Based upon what is known in literature, for KOH electrolyte the cathodic peak has been assigned to the formation of $Mn(OH)_2$ [6,7] and the corresponding anodic peak at −138 mV to the oxidation of $Mn(OH)_2$ to a variety of Mn^{3+} intermediates, including γ-Mn_2O_3, γ-MnOOH and β-MnOOH [6–8]. The reduction/oxidation processes for MnO_2 in aqueous KOH are not reversible, and hence the MnO_2/KOH system could only be used for non-rechargeable batteries. For LiOH electrolyte, we have assigned the peak at −480 mV to the formation of lithium intercalated Li_xMnO_2 phase and the corresponding anodic peak is reverse of this reaction. As noted earlier MnO_2 in aqueous LiOH can withstand repeated reduction/oxidation (Fig. 2) and hence has the potential for being used as a cathode material in rechargeable batteries.

In order to determine the products formed during reduction of MnO_2 in both LiOH and KOH electrolyte, the products were characterized by XRD and SEM analysis. The data is shown in Figs. 5–9. Fig. 5 compares the XRD patterns of the γ-MnO_2, before reduction Fig. 5a, and of the material formed on its reduction in LiOH (Fig. 5b) and in KOH (Fig. 5c). The material before reduction showed diffraction lines, characteristic of γ-MnO_2, at the 2θ angle of 16.3, 19.7 and 29.7. A small peak at 31 which is characteristic of diffraction line for β-MnO_2 [9] is also seen indicating that the materials contained some contamination of β-MnO_2 phase. As can be seen in Fig. 5b, the reduction of γ-MnO_2 in LiOH resulted in elimination of the γ-MnO_2 diffraction pattern (2θ = 16.3, 19.7 and 29.7). Only one peak at 2θ = 31.2 emerged. Thus, it could be concluded from these results that the discharge process completely changed the structure of the starting γ-MnO_2 material. The peak at 3.32 Å could be assigned to lithium intercalated (Li_xMnO_2) material. This is similar to that reported for γ-MnO_2 in non-aqueous lithium cells by Aurbach and co-workers [10]. However, in the case of KOH electrolyte, Fig. 5c, all the characteristic peaks for γ-MnO_2 remained unchanged except for a slight shift to lower 2θ values. Cedar and co-workers [11] have explained this in terms of the difference in the ionic size of the Li^+ and K^+ ions. As can be seen in Fig. 6, the γ-MnO_2 is an inter growth of ramsdellite (R) and pyrolusite (P). The $Mn(IV)O_6$ octahedra of ramsdellite are linked into double chains, each of which consists of two adjacent single chains that share octahedral edges [10,11]. These double chains having tunnels with rectangular-shaped cross sections accept the A^+ (A = Li)

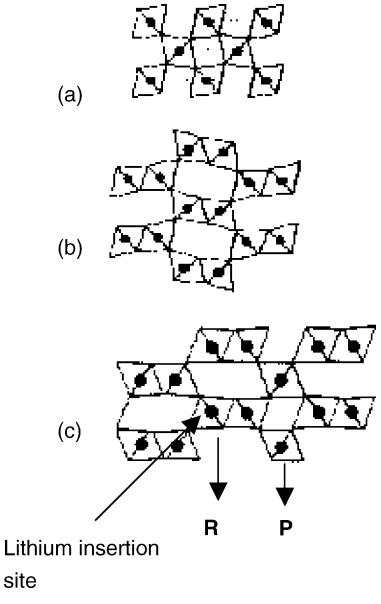

Fig. 6. Schematic diagram of the (a) P: pyrolusite, (b) R: ramsdellite and (c) γ-MnO_2, an inter growth between ramsdellite (R) and pyrolusite (P) shown in (0 0 1) plane.

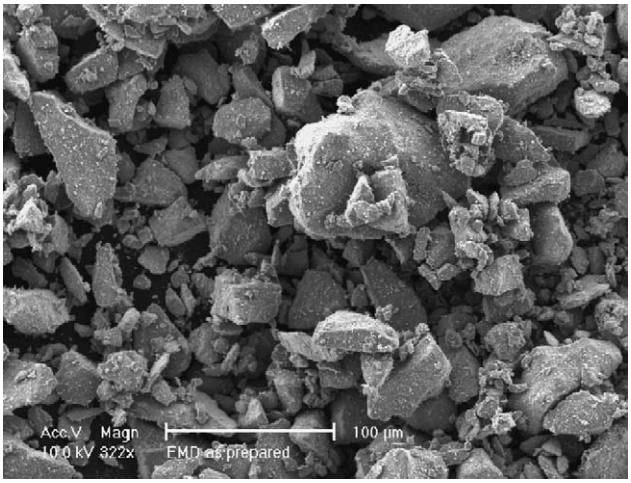

Fig. 7. SEM micrograph of the γ-MnO_2 cathode (as-received from Sigma–Aldrich).

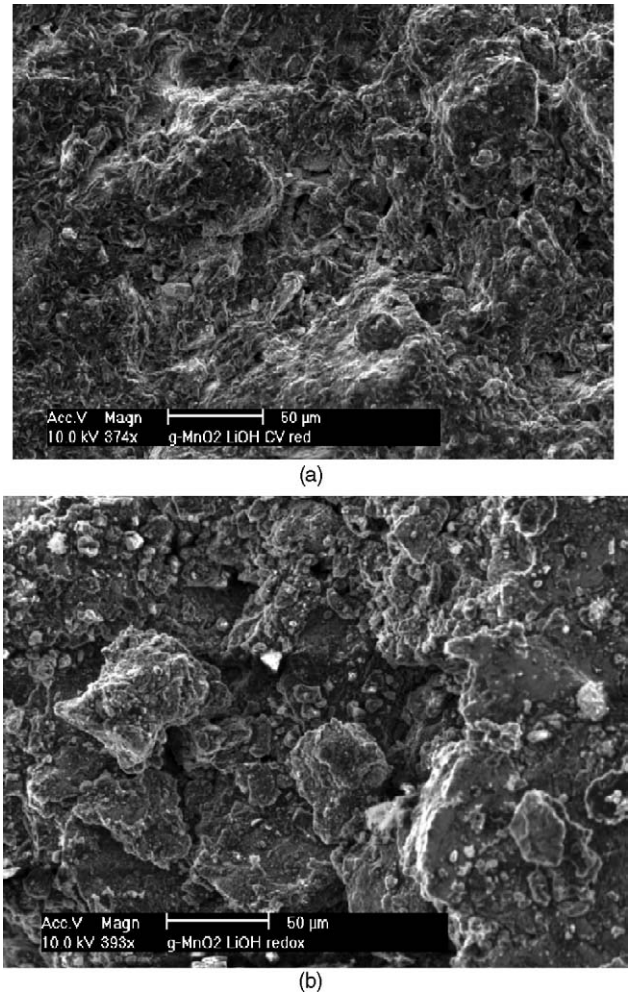

Fig. 8. SEM images of the γ-MnO_2 cathode (a) after reduction at −480 mV and (b) after oxidation via cyclic voltammetry in LiOH media.

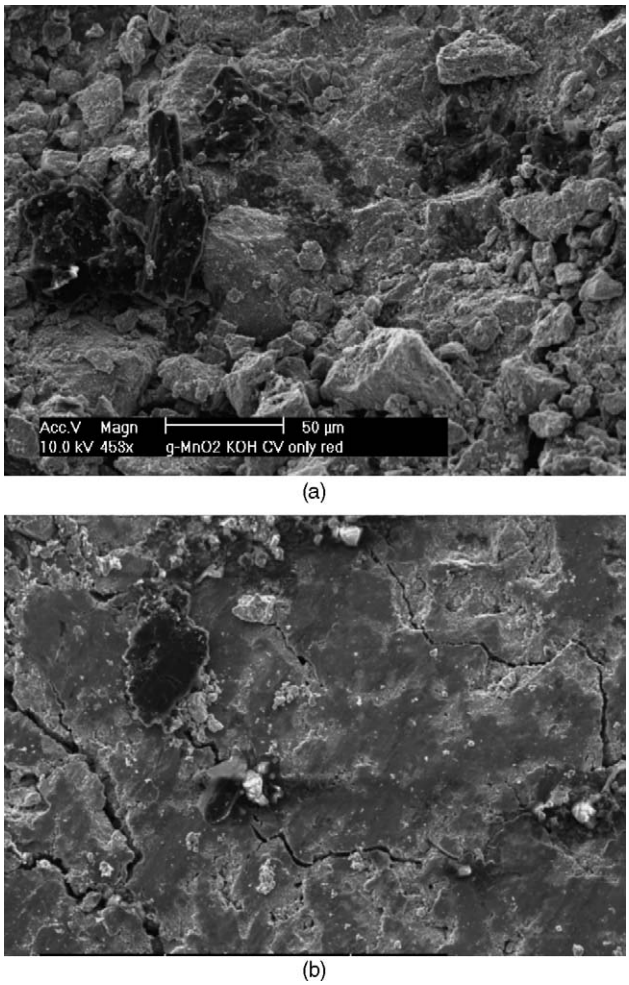

Fig. 9. SEM images of the γ-MnO_2 cathode (a) after reduction at −584 mV and (b) at oxidation via cyclic voltammetry in KOH media.

cation, which is approximately the same size as that of Mn, the columbic interactions dominate and hence the structure is stable for insertion/extraction of lithium ions. However, the size of the K^+ ion is twice as that of Li^+; therefore, the insertion site in Fig. 6 is not stable as the electrostatic energy of the structure is diminished. Hence, unlike for Li^+ the intercalation of K^+ is not possible in the γ-MnO_2 structure.

The surface morphologies of the materials formed during reduction and oxidation of γ-MnO_2 in LiOH and KOH electrolytes were determined by scanning electron microscopy. The SEM micrograph of the γ-MnO_2 before subjecting to reduction/oxidation is shown in Fig. 7. As can be seen from this micrograph, the material was crystalline of particle size 20–25 μm. The new phase (Li_xMnO_2), which was formed on reduction, Fig. 8a, had a much finer particle size (5–7 μm) compared to the original material. The subsequent oxidation of the reduced material produced a phase (Fig. 8b) whose characteristics were quite similar to that of the original γ-MnO_2 (Fig. 7). This particle size was 15–20 μm. Thus, the reduction/oxidation was almost reversible. This contrast with the material formed after reduction/oxidation cycle of γ-

MnO_2 in KOH (Fig. 9a and b). As can be seen in KOH the γ-MnO_2 underwent an irreversible change during the cycle.

4. Conclusions

Cyclic voltammetry coupled with X-ray diffraction and scanning electron microscope has been used to investigate structural changes that occur when manganese dioxide is electroreduced and subsequently oxidized. It is found that the reduction of γ-MnO_2 in LiOH produces a new phase of Li_xMnO_2, which is reversible. This differs from the mechanism reported in the literature for reduction/oxidation of the same material in aqueous KOH electrolyte. The difference in the mechanism through which reduction/oxidation of MnO_2 occurs can be explained in terms of the relative ionic sizes of Li^+ and K^+ ions. The Li^+ ions being comparable in size to Mn^{4+} could be intercalated into the octahedral structure of γ-MnO_2.

Acknowledgements

One of the authors (M. Minakshi) is grateful to Murdoch University for a research scholarship. The financial support of Australian Institute of Nuclear Science and Engineering (AINSE) to carry out some work at Australian Nuclear Science and Technology Organization (ANSTO) is also acknowledged. The author (M. Minakshi) would like to thank Ken Seymour, Stewart Kelly and Peter Fallon, all of Murdoch University for their technical support in carrying out some of the experiments.

References

[1] M. Minakshi, P. Singh, T.B. Issa, S. Thurgate, R. De Marco, J. Power Sources 130 (2004) 285–289.
[2] M. Minakshi, P. Singh, T.B. Issa, S. Thurgate, R. De Marco, Proceedings of the 41st Conference on Power Sources, Philadelphia, 2004, pp. 302–305.
[3] A. Kozawa, R.A. Powers, J. Electrochem. Soc. 113 (1966) 870; A. Kozawa, R.A. Powers, J. Electrochem. Soc. 115 (1968) 122.
[4] K. Kordesch, J. Gsellmann, M. Peri, K. Tomantschger, R. Chemelli, Electrochim. Acta 26 (1981) 1495.
[5] S. Fletcher, J. Galea, J.A. Hamilton, T. Tran, R. Woods, J. Electrochem. Soc. 133 (1986) 1227.
[6] J. Mc Breen, Electrochim. Acta 20 (1975) 221.
[7] J. Mc Breen, J. Power Sources 5 (1975) 525.
[8] S.W. Donne, G.A. Lawrence, D.A.J. Swinkels, J. Electrochem. Soc. 144 (1997) 2954.
[9] JCPDS card: 24-735.
[10] E. Levi, E. Zingrad, H. Teller, M.D. Levi, D. Aurbach, E. Mengeritsky, E. Elster, P. Dan, E. Granot, H. Yamin, J. Electrochem. Soc. 144 (1997) 4133.
[11] D. Balachandran, D. Morgan, G. Ceder, J. Solid State Chem. 166 (2002) 91.